Civil Engineering Infrastructures Journal 2025, 58(1): 71- 86
DOI: 10.22059/ceij.2024.360893.1928

RESEARCH PAPER

Comparison of Conventional and Energy Method in Evaluating the Seismic Fragility of Reinforced Concrete Frames

Javaheri Tafti, M.[1] and Haji Safari, M.[2*]

[1] Assistant Professor, Department of Civil Engineering, Taft Branch, Islamic Azad University, Taft, Iran.
[2] Ph.D. Candidate, Structural and Earthquake Research Center, Taft Branch, Islamic Azad University, Taft, Iran.

Received: 15 Jun. 2023; Revised: 20 Oct. 2023; Accepted: 08 Nov. 2024

ABSTRACT: This investigation aims at studying the energy method in calculating the exceedance probability of structures under seismic loads in reinforced concrete frames and its comparison with the conventional approach based on maximum story drift in structures. To do so, two reinforced concrete moment resisting frames with six and ten stories are designed based on the Iranian seismic code of practice and modeled nonlinearly with Perform software. Twenty near-fault earthquake records have been utilized to conduct the fragility analysis. The Incremental Dynamic Analysis (IDA) approach is used for the analysis and the IDA curves obtained from two methods are extracted and compared. The IDA curves resulted from the energy method provide this ability to calculate the elastic and plastic behavior zone and the instability point of the structure accurately. The output of the fragility analysis in reinforced concrete frames illustrates that the energy method can be utilized as an applicable approach in estimating the seismic fragility of the structures. The exceedance probability calculated in this approach is lower than the conventional method. The conventional method provides more conservative results in comparison to the energy method.

Keywords: Reinforced Concrete Moment Resisting Frame, Fragility Analysis, IDA Curve, Energy Method.

1. Introduction

There are various parameters to evaluate the behavior of structures. Parameters of displacement, rotation of plastic hinge, base shear, energy, etc., quantitatively and one-dimensionally express a seismic behavior. Fragility curves probabilistically express the behavior of the structure and exceed their performance levels.

The fragility curve defines the probability of exceeding an engineering demand parameter (such as drift) under specified boundary conditions (such as life safety) at different intensities of seismic loads (such as peak acceleration (Giordano et al., 2021; Hosseinlu et al., 2025).

Iteration of these operations for various seismic intensities or other single parameters would lead to normalized curves so-called fragility curves (Ge et al., 2021). Eq. (1) proposed by Barron-Corvera (2000) is used to demonstrate the conditional probability of exceeding the seismic

* Corresponding author E-mail: hs_m44@yahoo.com

response of the structure (R) from a particular performance limit state which is depicted by r_{lim} and is dependent on earthquake intensity (I):

$$\text{Fragility} = P\{R \geq r_{lim}|I\} \quad (1)$$

After choosing a few records in the IDA analysis approach, each of these records is scaled to specific intensities with equal steps and is exerted to the structure (Moradpour and Dehestani, 2021). The maximum dynamic response of the structure (usually the maximum drift) is extracted and creates the IDA curves with the maximum intensity corresponding to the earthquake records (Liu et al., 2021).

In a specific seismic load intensity (e.g. spectral acceleration, Sa) IDA curve suites illustrate the number of records by which the intended limit state is secured and the records by which the structural response has exceeded the limit state (Tavakoli et al., 2022). Fragility curves for structures have been developed with this argument (Afsar Dizaj and Kashani, 2022; Mesr and Behnamfar, 2023). In most previous studies, the maximum story drift parameter is considered as (R) or the Engineering Demand Parameter (EDP) and Immediate Occupation (IO), Life Safety (LS) and Collapse Prevention (CP), and limit states are assumed as r_{lim} (Moradi et al., 2022).

For instance, Xu and Gardoni (2016) probabilistically investigated the seismic fragility of reinforced concrete structures based on the maximum story drift and in various Sa intensities. Jalayer et al. (2015) developed the fragility of various structures using maximum story drift and PGA parameters as the structural response and seismic load intensity based on the linear regression method. Hancilar and Caktı (2015) conducted a research on the most suitable pair of earthquake intensity-engineering parameters in reinforced concrete structures. They concluded that the earthquake intensity-maximum story drift has better efficiency than other pairs of parameters. Del Gaudio et al. (2019) studied the drift fragility functions equation by estimating the damage in reinforced concrete structures under seismic load. They proposed a damage function based on the drift fragility approach. Hosseinpour and Abdelnaby (2017) studied the fragility of reinforced concrete structures under consecutive earthquakes using maximum story drift.

As it is obvious from the aforementioned studies, using story drift parameter as the EDP and limit states criteria proposed by regulations such as HAZUS and FEMA is a common and simple method in evaluating the fragility of structures (FEMA-356, 2000; Kircher et al., 2006). Moradi and Abdolmohammadi (2020) proposed an energy-based method in their study in which the dissipated plastic strain energy was used in the structure instead of using drift as EDP. They proposed that the Housner method can also be used to secure the limit states related to collapse prevention and life safety levels.

It was also illustrated that the elastic limit state and instability point can be determined by the energy method (Housner, 1960; Moradi and Abdolmohammadi, 2020).

Although the method of Moradi and Abdolmohammadi (2020) has been presented for a tall steel structure, the current study intends to assess this method on reinforced concrete structures and compare the fragility curves proposed by Moradi and Abdolmohammadi (2020) with the maximum story drift method to study whether it is possible to use this approach to evaluate the fragility curves of moderate and tall reinforced concrete structures or not. To do so, two reinforced concrete frames including six and ten stories are considered and the IDA curves from the maximum drift and strain energy are extracted and compared.

Eventually, the fragility curves for various limit states are calculated and compared through conventional and energy methods for these structures to evaluate the efficiency of the energy method in

determining the fragility of reinforced concrete frames.

2. Energy Balance

Earthquake is energy and in fact, during an earthquake, a large amount of energy reaches the structure. This energy, which is associated with ground shaking, causes vibration in the structure. Although force-displacement relationships (force balance) can also be used to investigate the dynamic response of the structure, but considering that earthquakes have an energetic nature, investigating this phenomenon with energy methods can be more useful. Nowadays, various methods are available for the analysis and design of structures, which one of them is the energy method. A structure would remain stable in case that the input energy (E_i) makes a balance with the internal energies in that structure (Moradi and Tavakoli, 2020). The internal energy in a structure consists of various energies including kinetic energy (E_k), dissipated energy through damping (E_i) and strain energy resulted from deformations.

The strain energy in a structure can be separated into potential energy (absorbed energy) (E_e) and dissipated energy (E_{in}) with respect to the deformation values (Goodarzi et al., 2023). The strain energy in the structure would be in form of absorbed energy if the deformations are within the elastic range and the strain energy would be the sum of potential and dissipated energy in the case that the deformations are within the plastic range.

Therefore, the energy balance in a structure can be defined as Eq. (2):

$$\begin{aligned} E_i &= E_k + E_{£} + E_e + E_{in} \\ E_k &= \frac{1}{2m\dot{u}^2} \\ E_{£} &= \int C\dot{u}^2 dt \\ E_e + E_{in} &= \int f_s du \\ E_i &= -\int m\ddot{u}_g du_g \end{aligned} \quad (2)$$

where C: is related to the damping coefficient, m: is mass, f_s: is the force, $\dot{u}$: is the velocity, u: is the displacement of structure, $\ddot{u}$: is the acceleration of the mass, and t: is time. Moradi and Abdolmohammadi (2020) proposed that the (E_{in}) parameter can be utilized as an EDP to assess the fragility of a structure. The dissipated energy in a structure has a direct relationship with the destruction level in the structure. The more the dissipated energy resulted from the plastic deformations in the structure is, the more damage the structure would experience during the seismic load. They proposed that in the case of using the plastic strain energy as EDP, the Housner (1960) method can be used for computing the limit states. This method is described in Section 4.

3. Model Properties

Reinforced concrete frames are used to achieve the goals of this investigation. For this purpose, concrete structures with moment resisting frame system with moderate ductility are considered with six and ten stories exposed to gravity loads according to loading guidelines and lateral loads according to the Iranian seismic code of practice (Standard No. 2800) with the aid of equivalent static method (Moradi et al., 2019). The specifications of gravity loads are depicted in Figure 1 and it is considered that the structure is located in a region with a high level of seismicity (A = 0.3 g) and on a soil type III.

It is assumed for 3D modeling and design of the structure that the structure has 4 spans with a length of 5 m each in both directions. The plan of the studied structure is demonstrated in Figure 1.

Table 1. Gravity load specifications (Moradi et al., 2020)

Parameter	Value	Unit
Dead load	600	Kg/m^2
Live load	500	Kg/m^2
Roof dead load	650	Kg/m^2
Snow	150	Kg/m^2
Roof live load	200	Kg/m^2

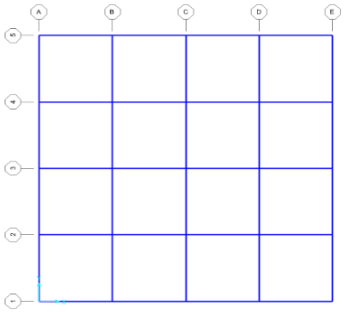

Fig. 1. Structural plan

After determination of gravity and lateral loads, the structure is modeled in SAP2000 v17 software and designed based on the Iranian concrete regulations and the required structural elements are achieved.

After computing the structural sections, the structure is controlled by checking some parameters such as relative inter-story drift. Furthermore, the materials specifications are illustrated in Table 2.

Table 2. Specifications of concrete and steel materials

Parameter	Value	Unit
Fc	2400000	Kg/m^2
Fy	34000000	Kg/m^2
Special weight	2400	Kgf/m^3

The structure is analyzed and designed after the modeling procedure and the specifications of sections for structural elements are depicted in Tables 3 and 4.

Table 3. Specifications of sections in the ten-story building

Story	Beam section	Column section
1-3	55×55	70×70 20 T 24
4-7	50×50	60×60 20 T 18
8-9	40×40	50×50 20 T 14

Table 4. Specifications of sections in the six-story building

Story	Beam section	Column section
1-3	50×50	60×60 20 fi 22
4-6	40×40	55×55 20 fi 16

After designing the structure and obtaining the sections, the middle frame of the plan is selected for conducting the nonlinear analysis and then the structure is modeled in Perform 3D software. The concentrated plastic hinge is used in defining the nonlinear behavior of the structure. It is considered that the structure has concentrated plasticity in critical regions and is elastic in other regions. The Iranian Guideline No. 360 is used for nonlinear modeling and the modeling values and acceptance criteria are selected based on this guideline. The behavior of structural elements in this model is according to the type of their internal work and the resulted force displacement curve is in form of force-controlled or displacement controlled condition. The force displacement curve can be an indication of ductile, semi-ductile or fragile behavior. The force-displacement curve in ductile behavior has four zones according to Figure 2a.

Finally, elastic and plastic values are combined and elements with elastic properties containing concentrated plasticity at the two ends are created. The modeled frames for six and ten-story structures are illustrated in Figure 3.

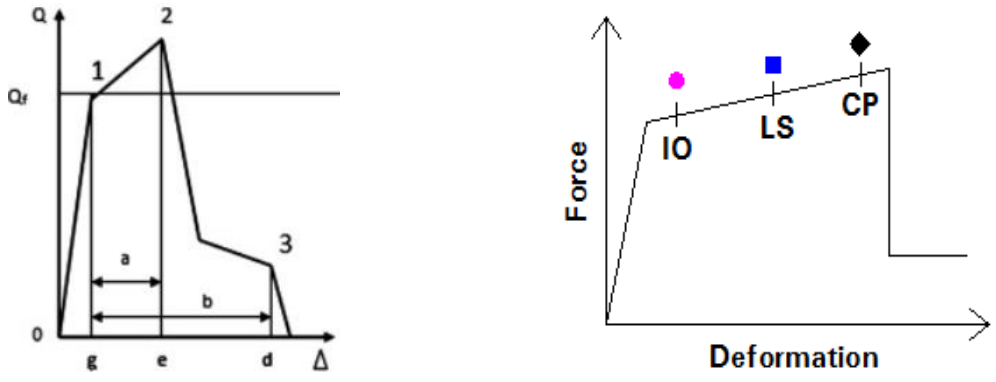

(a) **(b)**

Fig. 2. Force-deformation curve of the ductile element (Tavakoli and Afrapoli, 2018; Ugalde et al., 2019)

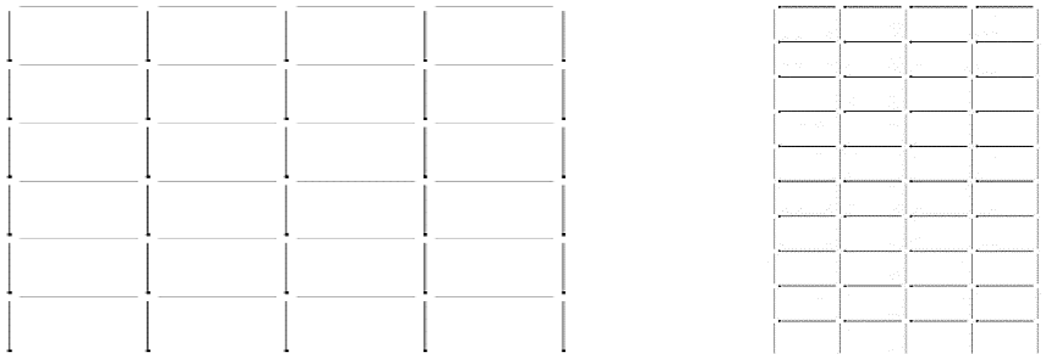

(a) **(b)**

Fig. 3. The modeled frames: a) Six-story frame; and b) Ten-story frame

4. Energy Method in Fragility Evaluation of the Structure

The steps of the approach proposed by Moradi and Abdolmohammadi (2020) for assessing the fragility of structures based on the plastic strain energy in the structure are presented in the following. In these steps, the required parameters for six and ten-story buildings are computed.

In various researches, many records have been used for IDA analysis. Generally, there are two methods for fragility analysis. Time history analysis and IDA analysis. In time history analysis, a larger number of records are used to perform the analysis and obtain the engineering demand parameter distribution.

In IDA analysis, a more limited number of records are used, but each record is scaled to many seismic intensities. IDA method has been used in this research. For this purpose, twenty seismic records have been used according to different references.

The AC parameter can be calculated based on Eq. (3) (Moradi and Abdulmohammadi, 2020).

$$E_t = \frac{1}{2} M S_v^2 = \frac{1}{2} M \left(\frac{T}{2\pi} S_a g \right)^2 \quad (3)$$

where M: is the structural mass, T: is period, S_a: is the spectral acceleration and g: is the gravity acceleration.

In various studies such as the report prepared by EERC in 1998, it was declared that the external work done by the system is equal to the elastic input energy multiplied by the energy modification factor (γ). γ: is dependent on ductility ratio (μ_s), ductility reduction factor (R_μ) and structural period (T) and is calculated as Eq. (4).

$$\gamma = \frac{2\mu_s - 1}{R_\mu^2} \quad (4)$$

where T_1 =0.57 and $T' = T_1 . \sqrt{2\mu_s - 1}/\mu_s$ since all the parameters in Eq. (3) are constant except S_a, the value of (E_t) can be readily determined if a specific S_a can be defined for each performance level. μ_s and R_μ are shown in Table 5.

Table 5. Ductility reduction factor and the corresponding structural period range (Moradi and Abdolmohammadi, 2020)

Period range	Ductility reduction factor
$0 \le T < \frac{T_1}{10}$	$R_\mu = 1$
$\frac{T_1}{10} \le T < \frac{T_1}{4}$	$R_\mu = \sqrt{2\mu_s - 1} . (\frac{T_1}{4T})^{2.513 \log(\sqrt{2\mu_s - 1})^{-1}}$
$\frac{T_1}{4} \le T < T'_1$	$R_\mu = \sqrt{2\mu_s - 1}$
$T' \le T < T_1$	$R_\mu = \frac{T\mu_s}{T_1}$
$T_1 \le T$	$R_\mu = \mu_s$

Since tall buildings period range is more than (T_1), the ductility reduction factor is considered equal to the ductility factor. According to the Iranian seismic code of practice, the S_a can be considered as AB for LS performance level wherein A is the maximum design acceleration and B is the building response factor. The S_a value in CP performance level can be considered as 1.5 times of the Spectral Acceleration (SA) in LS performance level. Parameter of calculating AC for six and ten-story buildings in LS performance level is illustrated in Table 6.

For the CP performance level, the (E_{in}) values for six and ten-story buildings are calculated as 72325 and 129011 kg.m, respectively. Assessing the exceedance probability by comparing Steps 3 and 4. For each performance level, the value of dissipated strain energy in a specific intensity of seismic load in the structure is compared to the amount of allowable strain energy and its exceedance probability is calculated. Returning to Step 3 and computing the exceedance probability for other seismic load intensities. There are measures such as SA, Spectral Displacement (SD), Maximum Displacement Velocity (PGV) and Maximum Ground Acceleration (PGA) to measure intensity. Each of these parameters has its own characteristics.

Since in the past research in the field of fragility assessment with energy method, spectral acceleration and spectral displacement criteria have been used, in this research, it has been tried to calculate fragility from the perspective of ground acceleration. There is many research in the field of fragility curve that evaluated the fragility based on the maximum acceleration of the ground.

5. Seismic Load

The incremental time-history analysis is used in the current study. Twenty near-fault earthquake records is selected based on the recommendation of FEMA P695 for IDA analysis (Council, 2009). The specifications of these records are illustrated in Table 7. Near field earthquakes refer to the points of the earth whose distance from the surface center of the earthquake is less than a certain limit? The characteristics of this type of earthquake include the effect of progression, relative amplitude, pulse period and the number of pulses in the speed record (Sharma et al., 2020).

6. Assessing the Seismic Performance of the Structure

After the initial modeling, the seismic performance of two frames is studied in this section. The horizontal displacement curve of the roof in six and ten-story frames in various maximum accelerations of the Loma earthquake record is illustrated in Figure 4. According to this Figure, as it is expected, maximum rood horizontal displacement in the structure increases by increasing the maximum acceleration imposed to the structure. Residual displacement is one of the most important parameters that can be achieved from the roof horizontal displacement curve.

Table 6. Parameters of calculating ac for six and ten-story buildings for the ls performance level

Parameters	Unit	10-Story	6-Story
Period	s	1.2	0.75
A	-	0.35	0.35
B	-	1.75	2.5
Sa	-	0.6125	0.875
μ_s	-	1.85	1.52
R_μ	-	1.85	1.52
M	Kg	105000	63000
E_t	Kg.m	71914.21	37204
γ	-	0.788897	0.88
$E_{in(LS)}$	Kg.m	56732.9	33070

Table 7. Records specifications (Moradi and Abdolmohammadi, 2020)

ID No.	Lowest frequency (Hz.)	Record information	PGA max (g)
1	0.13	IMPVALL/H-E06_233	0.44
2	0.13	IMPVALL/H-E07_233	0.46
3	0.16	ITALY/A-STU_223	0.31
4	0.15	SUPERST/B-PTS_037	0.42
5	0.13	LOMAP/STG_038	0.38
6	0.13	ERZIKAN/ERZ_032	0.49
7	0.07	CAPEMEND/PET_260	0.63
8	0.10	LANDERS/LCN_239	0.79
9	0.11	NORTHR/RRS_032	0.87
10	0.12	NORTHR/SYL_032	0.73
11	0.13	KOCAELI/IZT_180	0.22
12	0.08	CHICHI/TCU065_272	0.82
13	0.06	CHICHI/TCU102_278	0.29
14	0.10	DUZCE/DZC_172	0.52
15	0.06	GAZLI/GAZ_177	0.71
16	0.13	IMPVALL/H-BCR_233	0.76
17	0.06	IMPVALL/H-CHI_233	0.28
18	0.13	NAHANNI/S2_070	0.45
19	0.13	LOMAP/BRN_038	0.64
20	0.25	LOMAP/CLS_038	0.51

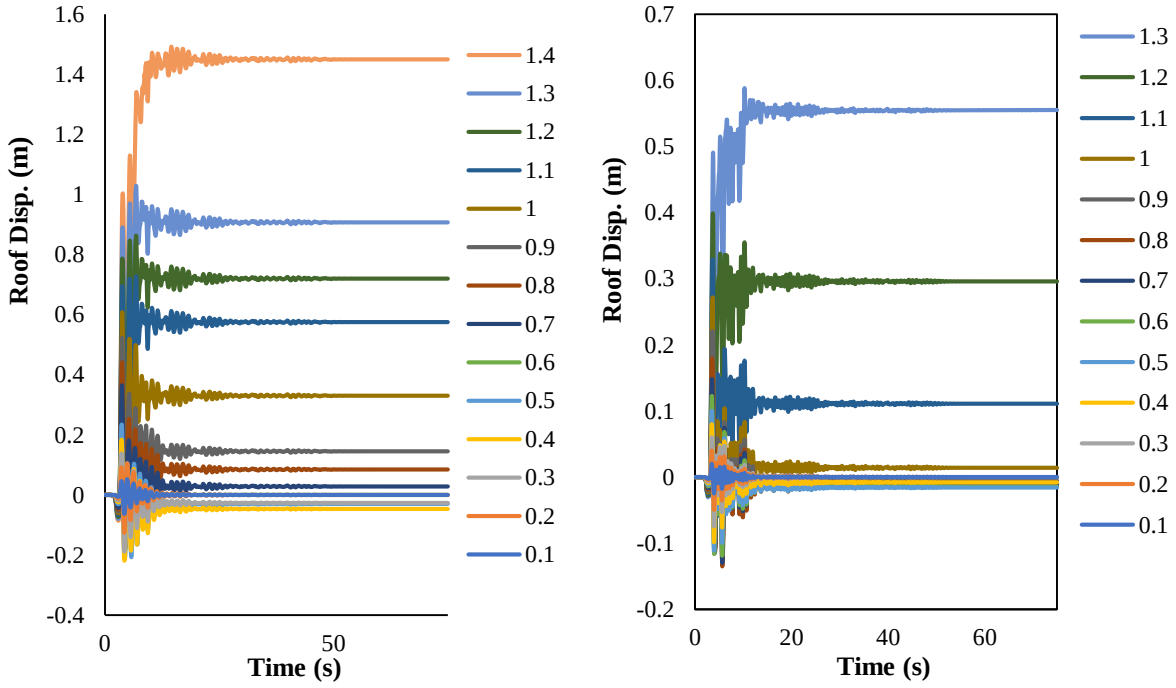

Fig. 4. Roof horizontal displacement: a) Ten-story building; and b) Six-story building

In the ten-story structure, the horizontal residual displacement remains zero until PGA = 0.6 g and increases hereafter. In the six-story building, the residual displacement remains zero until PGA = 0.5 g. Rising the residual displacement in the structure implies the growth of the dissipated plastic strain energy and damage in the structure.

The analyses results indicate that the residual displacement in the structures designed based on the Iranian seismic code of practice (standard 2800) occurs in the six-story building in a lower PGA in comparison to the ten-story structure. The time-history curve of the base shear in six and ten-story buildings is illustrated in Figure 5. Base shear is an indication of

structural capacity against seismic loadings. According to Figure 5, the base shear imposed to the ten-story structure is higher than that of the six-story structure and the maximum base shear of the structure increases by rising the PGA. The maximum drift curve of six and ten-story frames under Loma earthquake record is illustrated in Figure 6. In IDA analyses, the more the maximum story drift the structure has, the higher amount of response and performance would be in the structure. Based on the FEMA guideline, the values of 0.01, 0.02 and 0.04 as the drift limit are considered in IO, LS and CP performance levels. According to Figure 6, the amount of drift rises in the stories by increasing the maximum acceleration applied to the structure.

The maximum drift does not necessarily take place in a specific story in various maximum accelerations. For instance, in Figure 6a, the maximum story drift in the ten-story building occurs in stories 2-5 in various maximum accelerations while the maximum drift has taken place in stories 2 and 3 in the six-story building.

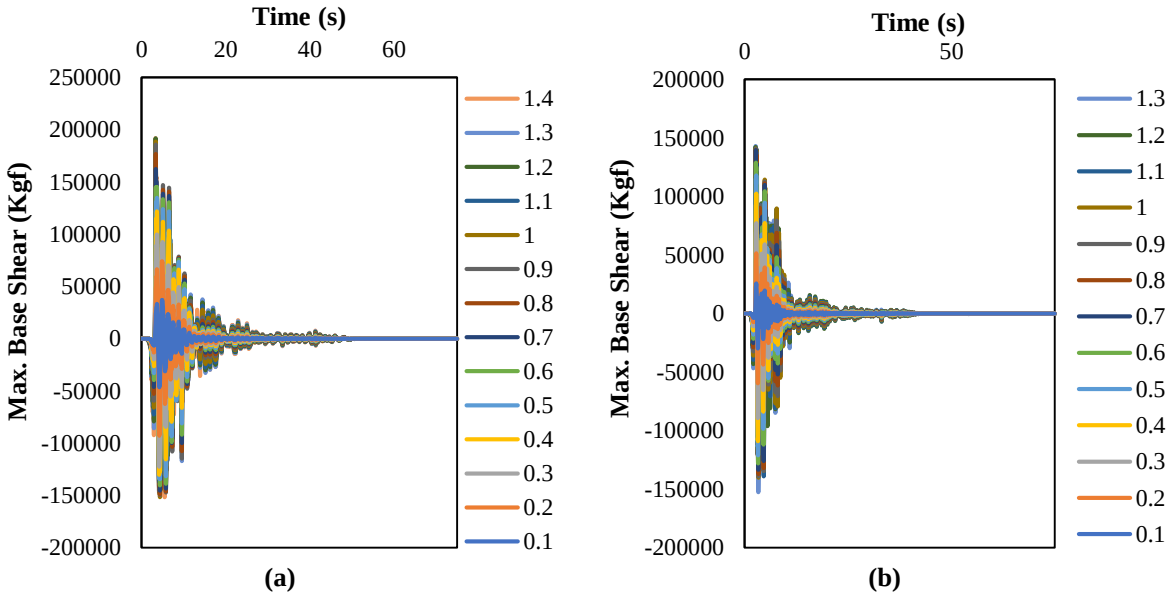

Fig. 5. Time-history curve of the base shear in the structure: a) Ten-story building; and b) Six-story building

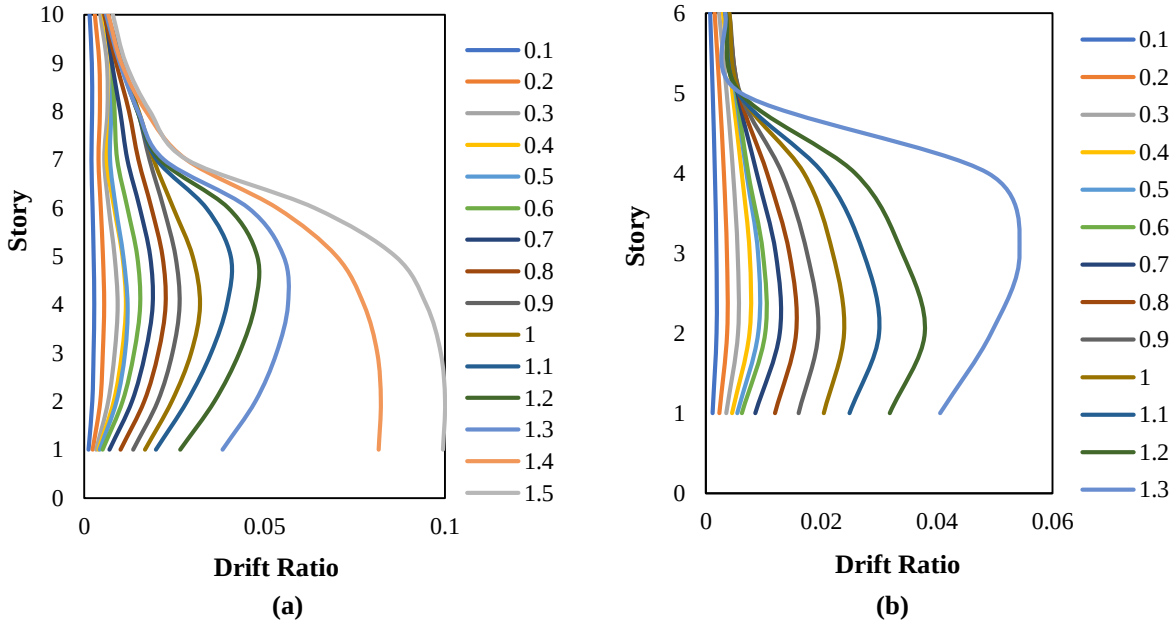

Fig. 6. The maximum drift curve of the structure: a) Ten-story building; and b) Six-story building

By applying the seismic load to the structure, the input energy should be equal to the internal energies in order to keep the stability of the structure. The input energy of the structure includes kinetic energy, absorbed strain energy, dissipated strain energy, and dissipated energy due to damping. The time-history curve of the energies for the six-story building in the maximum acceleration of 0.6 g is illustrated in Figure 7. The elastic strain energy starts from non-zero values with respect to this figure. This energy exists in the structure due to the gravity load and elastic deformations that occurred in the structure in form of potential energy before applying seismic load and increases by applying seismic load and making higher elastic deformations and its value fluctuates as far as the kinetic energy exists in the structure.

According to Figure 7, since the six-story building was not able to establish a balance in this maximum acceleration by kinetic and elastic energies and damping against the input energy due to the seismic load, the structure has employed its plastic strain energy capacity to create plastic deformations and the plastic strain energy has been formed in the structure. Based on Figure 7, the structure has been able to establish an energy balance against the input energy due to the seismic load by dissipating 8250 kg.m energy through plastic deformations, 3820 kg.m dissipated energy through damping, 5584 kg.m of elastic strain energy and 7027 kg.m of kinetic energy. To make the values of the dissipated strain energy in the structure meaningful, the plastic hinge rotation performance in the six-story structure under the Loma earthquake record in the maximum acceleration of 0.6 g is illustrated in Figure 8. According to this figure, no rotation is formed in the LS performance level in the structure and only a few beams have reached or exceeded the IO performance level (between IO and LS performance level).

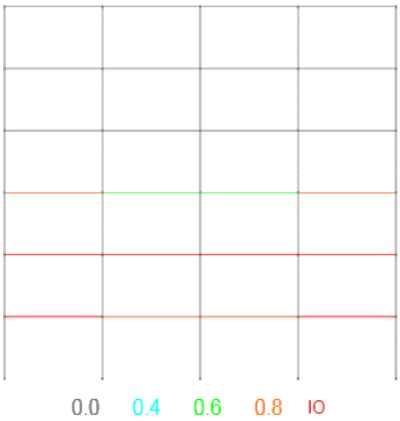

Fig. 7. Structural performance of the six-story building under Loma record with 0.6 g maximum acceleration

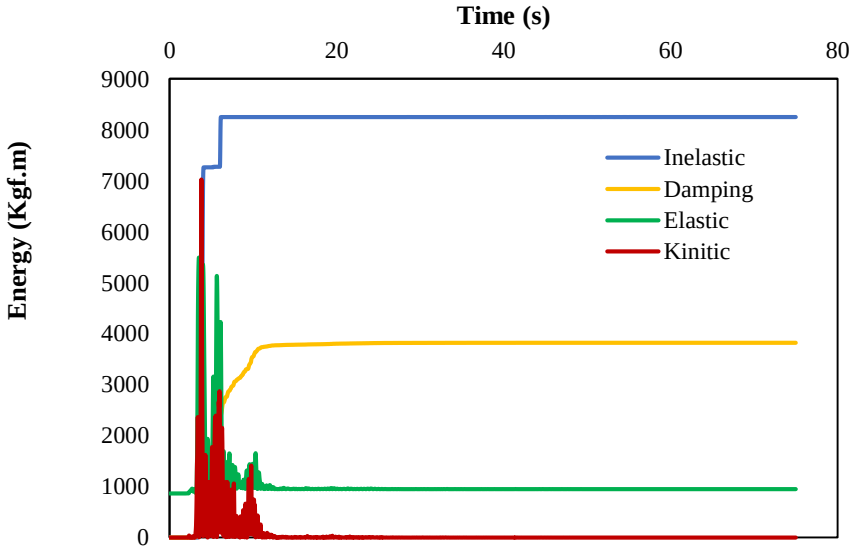

Fig. 8. Time-history curve of the internal energy in the six-story building under Loma record with PGA = 0.6 g

The time-history curve and performance of plastic hinges of the ten-story structure under the Loma earthquake record with the maximum acceleration of 0.7 g are also illustrated in Figures 9 and 10. The plastic strain energy in the structure indicating the measure of nonlinear deformations and damage exerted to the structure. The more the plastic strain energy is in the structure, the higher the damage and plastic hinge rotation would be in the structure. The time-history curve of plastic strain energy in six and ten-story buildings under the Loma earthquake record in various maximum accelerations is demonstrated in Figure 11.

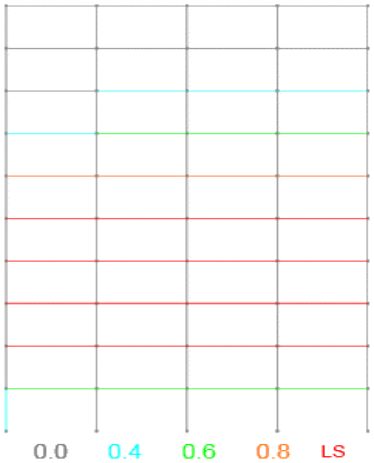

Fig. 9. Structural performance of the ten-story building under loma record with 0.7 g maximum acceleration

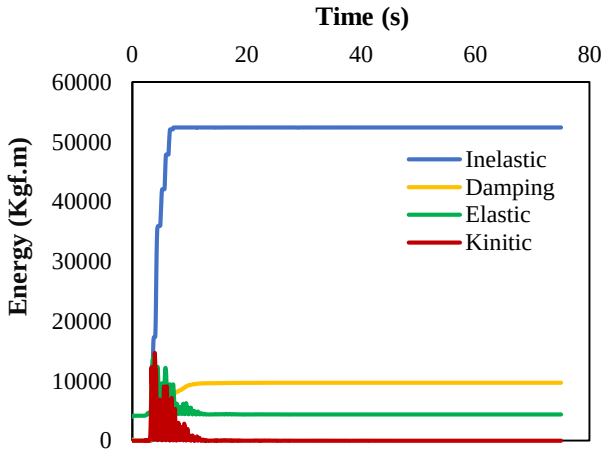

Fig. 10. Time-history curve of the internal energy in the ten-story building under Loma record with PGA = 0.7 g

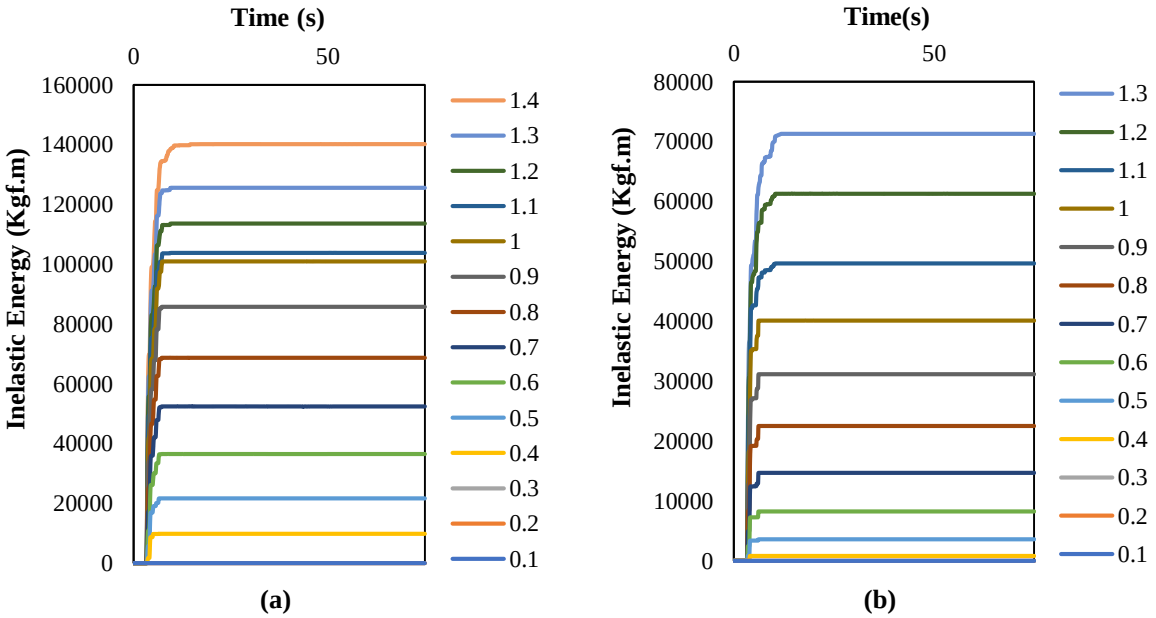

Fig. 11. Time-history curve of the plastic strain energy under Loma earthquake record in: a) Ten story; and b) Six story structures

According to Figure 11, the plastic strain energy measure in the structure increases by the rise of the acceleration value applied to the structure. These curves depict the amount of cumulative dissipated strain energy in the structure indicating the amount of energy dissipated in the structure until the x moment. Therefore, the time-history curve of the plastic strain energy in the structure has an ascending trend showing the amount of energy dissipated in a particular moment in the structure.

Roof displacement, base shear, maximum story drift and plastic strain energy parameters are studied in the structure, each of which can be used as EDP in assessing the fragility of the structure. The IDA and fragility curves of six and ten-story structures are calculated and compared in the following by considering the maximum base shear and plastic strain energy as EDP.

7. Incremental Dynamic Analysis

The IDA curves of six and ten-story buildings under specific earthquake records are illustrated in Figure 12 for the case that the maximum drift is considered as EDP. The PGA is used as IM with 0.1 g steps to conduct the IDA analysis and the analysis process continues if the drift reaches 0.1.

This form of presenting the IDA curves is a common method that is generally investigated before the fragility curve. This curve represents the variation trend of the structural maximum drift from lower values of IM until the instability moment. The IDA curves are presented in this section by considering the plastic strain energy as EDP for the studied structures. These curves are presented for six and ten-story buildings in Figure 13.

For a better evaluation of the IDA curves resulted from drift and energy methods, the curves achieved from the Imperial Valley earthquake record in the ten-story structure are separately compared (Figure 14). The IDA curves obtained from these two methods have the following differences:

- The IDA curve of the energy method starts from zero points however does not increase by the rise of acceleration and remains constant until a specific amount of acceleration. The zero value of the plastic strain energy in the structure illustrates that the structure has a perfectly elastic behavior and nonlinear deformations have not taken place in the structure while the IDA curve resulted from the drift method starts from zero and rises by increasing the acceleration. This curve has a linear behavior until a specific acceleration and exits the linear behavior hereafter.

Exceeding the linear state does not mean the exit of the elastic condition for this curve because the structure can become roughly nonlinear before this point but this curve cannot show the acceleration in which the structure enters the nonlinear condition.

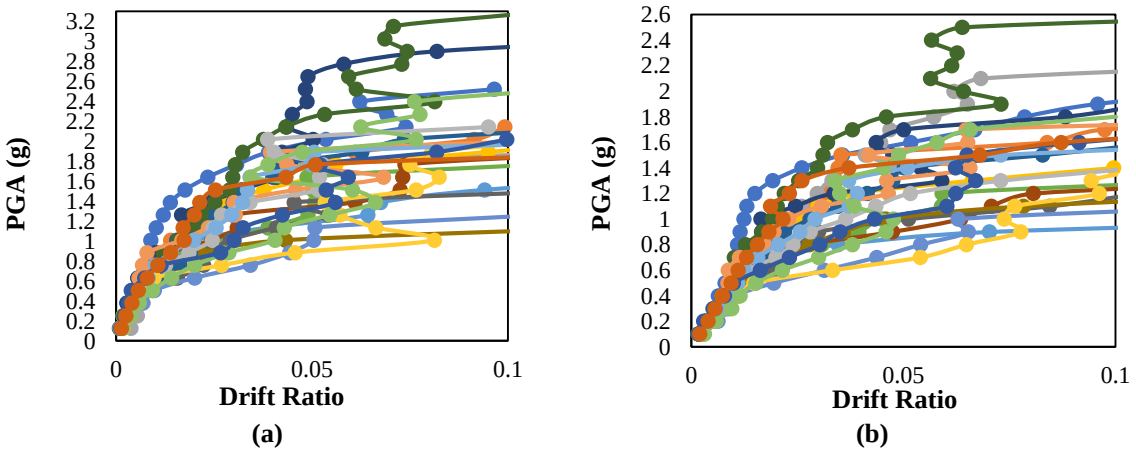

Fig. 12. IDA curve of the structures by considering the maximum drift as EDP: a) Ten-story building; and b) Six-story building

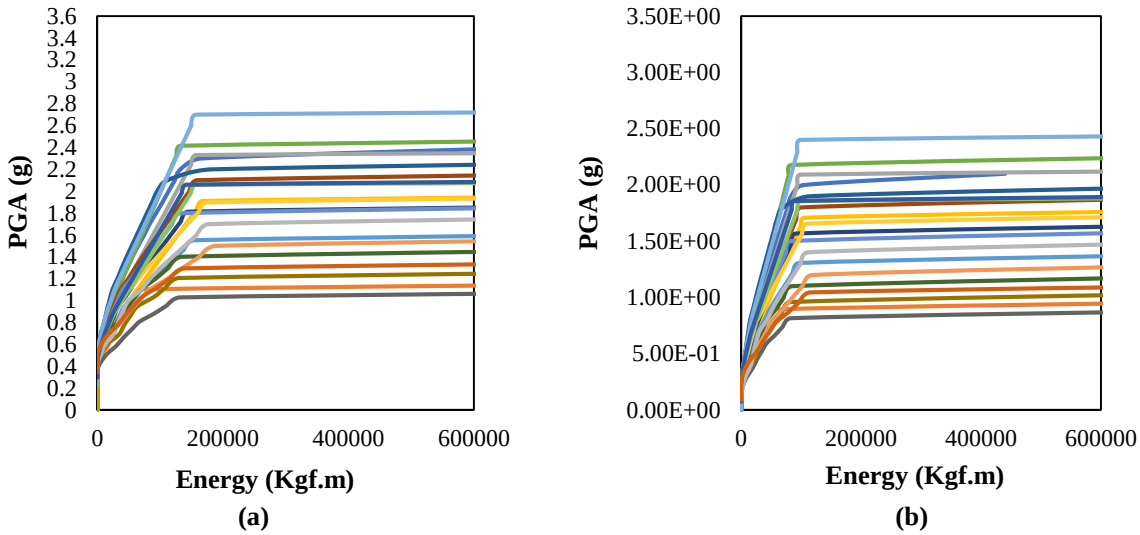

Fig. 13. IDA curve of the structures by considering the plastic strain energy as EDP: a) Ten-story building; and b) Six-story building

- The IDA curve obtained from the energy method after the elastic region (zero value) illustrates that the structure enters plastic deformations. After the elastic point, this curve would have an ascending trend and would never be constant or descending because by increasing the input energy, the structure is obliged to dissipate more plastic strain energy to reach equilibrium.

However, the IDA curve achieved from the drift method may not have an upward trend after the linear region and remain constant or have a downward trend. The reason for this phenomenon might be the occurrence of soft-story or changing the maximum drift of the structure from one story to another. However, these two curves in high accelerations in which the structure would reach the instability have a similarity. The energy and drift values would surge in the structure by increasing one or few acceleration steps. This immediate increase in drift or plastic strain energy can be described as the global instability of the structure. In most earthquakes selected in this study, instability point in two IDA curves corresponds with each other; however, there have been some records in which this point has discrepancies.

In this situation, the drift value has net reached 0.1 with an abrupt increase of the energy; in other words, the energy has not increased abruptly by reaching the drift to 0.1 value. Elastic points, performance levels calculated with drift and energy methods for the ten-story building and the instability point of the structure are illustrated in Figure 14.

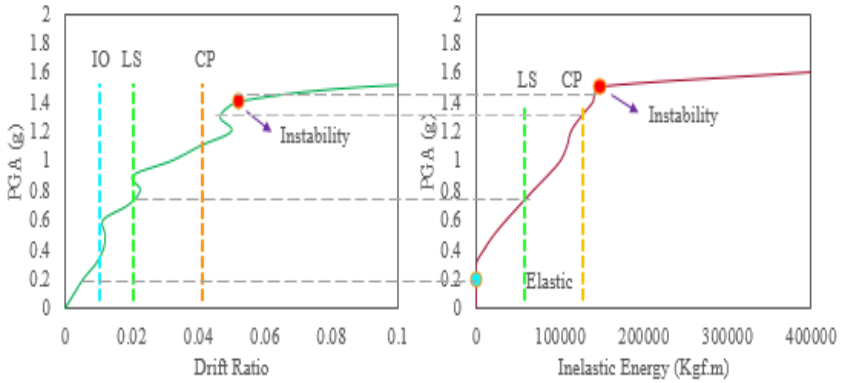

Fig. 14. Comparison of IDA curve under Imperial Valley record in ten-story building with drift and energy methods

The horizontal gray dash line in Figure 14 shows the comparison of elastic, LS, CP and instability points compared to the drift approach. These two methods present the same instability point in this specific record. The elastic performance level occurs in acceleration lower than the IO performance level. The highest difference in IDA curves in this record has taken place in CP performance level.

This level occurs in 1.3 g acceleration in the energy method and in 1.1 g in the drift method in the structure. The fragility curves of six and ten-story buildings with two different methods are compared in the following in order to examine the differences of these two methods in various performance levels.

8. Fragility Analysis

Fragility curves of the 2D frame of the ten-story reinforced concrete frame with two methods of drift and dissipated strain energy are illustrated in Figure 15. In this figure, the points are related to the exceedance probabilities which are calculated in various performance levels and the lines are related to the fitted curves with normal distribution function. The exceedance probability from elastic, LS, CP and instability are presented in the energy method while the exceedance probability from IO, LS, CP and instability is calculated in the drift approach.

For a better comparison, maximum acceleration values related to the 50% exceedance probability in various performance levels are compared. Maximum accelerations that show the 50% exceedance probability in three levels LS, CP and instability in drift method are 0.95 g, 1.35 g and 1.8 g, respectively. In this research, which is based on the energy method, it has been tried to express IDA curves based on the maximum acceleration of the ground (as a measure of intensity) and the plastic strain energy dissipated in the structure (as a parameter of engineering demand). In both methods, intensity measure is considered based on the maximum acceleration of the ground. This parameter is common in both methods.

For example, the IDA curve starts from zero by the drift method and increases immediately with the increase in the intensity of the seismic load. But in the energy method, up to a certain intensity, the value of the IDA curve is equal to zero. On the other hand, the performance levels obtained from two methods (such as LS and CP) have also been compared, which can be considered as a benchmark for comparison.

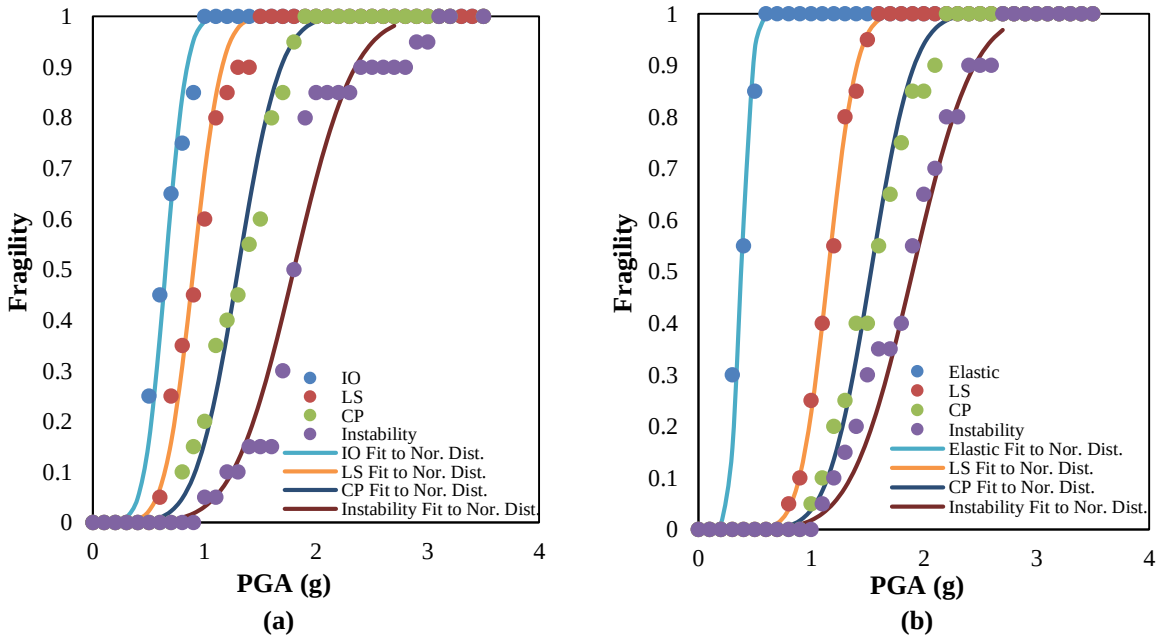

Fig. 15. Fragility curve of the ten-story structure with: a) Drift method; and b) Energy method

These values in the energy method are equal to 1.15 g, 1.52 g and 1.85 g, respectively. As it can be observed, the results achieved from the drift approach are more conservative than the energy approach. The fragility curves for the six-story building with drift and plastic strain energy have been illustrated in Figure 16. The maximum accelerations that show the 50% exceedance probability from three performance levels of LS, CP and instability point in the drift method are calculated as 0.7 g, 1.05 g and 4.5 g, respectively. These values for the energy approach are 0.85 g, 1.35 g and 1.55 g, respectively. As it is depicted, the exceedance probability resulted from the energy approach presents higher values in comparison to the drift method in the six-story building.

One of the advantages of the energy method compared to the drift method is that the exceedance probability from the elastic level can be calculated in the structures. Therefore, this method can be used for the structures for which the design seismic load is required to remain within the elastic range. For instance, the maximum exceedance probability (100%) from the elastic performance level in six and ten-story buildings takes place in the maximum acceleration of 0.4 g and 0.6 g, respectively, whereas the maximum exceedance probability from the IO performance level in these structures occurs in maximum accelerations of 0.7 g and 0.9 g, respectively. The ability to calculate the exceedance probability from the elastic level in structures is one of the advantages of this approach. The main limitation of this method is in evaluating the boundary conditions related to different performance levels.

Although the energy method is considered an excellent and perfect method in evaluating the probability of exceedance the elastic level, it can be associated with errors in other levels. In past research, Housner (1960) relationship has been used to calculate different levels of performance. Although this method is known as a definite and well-known method in the design of structures with energy methods, it can also be associated with errors in the evaluation of fragility curves. This method provides the amount of plastic strain energy at the design level. The main hypothesis of the energy method is that this input energy can make the structure reach the LS performance level. The same issue can be considered uncertainty in fragility assessment with the energy method.

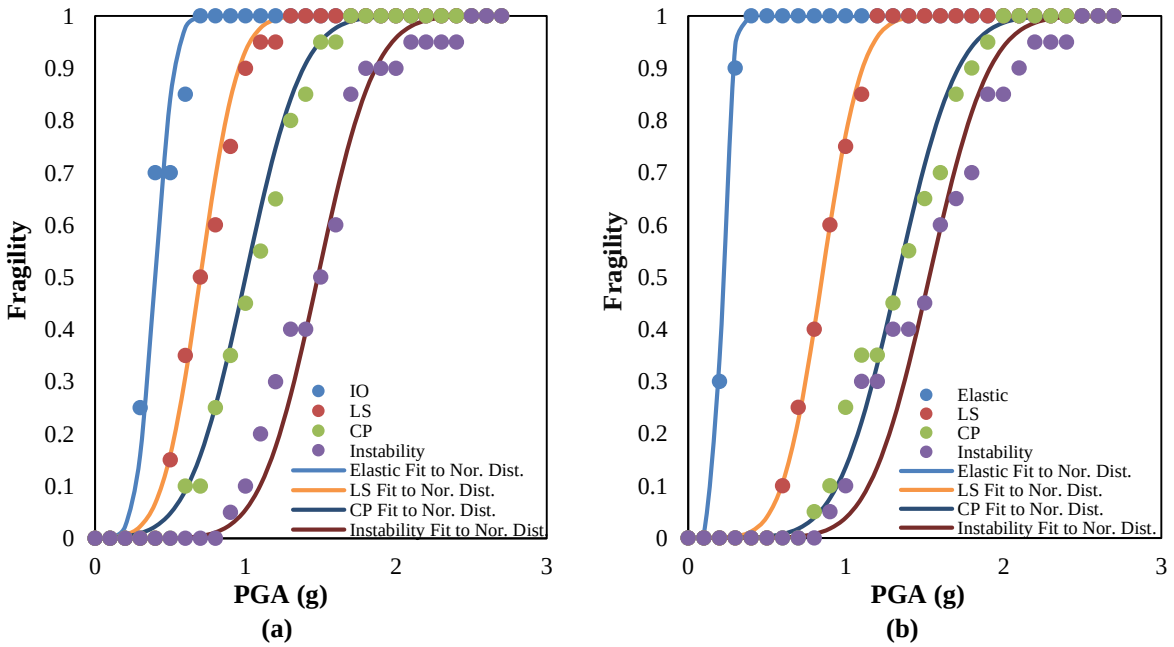

Fig. 16. Fragility curve of the six-story structure with: a) Drift method; and b) Energy method

The energy method has been proposed as a new method in assessing the fragility of structures. Structural design methods are changing from force methods to performance methods (Gardner, 2019). One of these performance methods is energy-based design. When the energy-based design method, which is considered as an efficient method, is included in the regulations, the energy-based fragility assessment method will be the most important tool for fragility analysis.

9. Summary and Conclusion

The aim of this study was to compare the fragility of six and ten-story reinforced concrete frames with the conventional and energy methods and to evaluate the possibility of using the energy method for reinforced concrete structures with moderate and short height. To do so, the seismic performance of frames was firstly studied. Then, the energy balance of internal and input energy due to seismic load was investigated. Afterward, the IDA curves based on energy method and inter-story drift were calculated and presented and their differences were discussed. At the end, the fragility of the frames was calculated for elastic, LS, CP and global instability damage levels in the energy method and compared with IO, LS, CP and global instability levels in the drift method.

The summary of the results are presented as follows:

- The maximum exceedance probability (100%) from the elastic performance limit in six and ten-story frames occurred in the maximum acceleration of 0.4 g and 0.6 g, respectively.
- Using the energy method represents higher values of fragility in a particular maximum acceleration compared to the drift method. In other words, the seismic fragility of the structures in the conventional method is more conservative than the energy method.
- The IDA curve resulted from the energy method is a curve with an ascending trend. This curve can obviously represent the performance point of the structure in the elastic zone.
- Since the drift value is the criterion of most guidelines in assessing the fragility of the structures, Ls and CP performance levels in the energy method can be transmitted to the drift method by modifying the Housner (1960) method and applying reduction factors which can be considered for further investigations.

10. References

Afsar Dizaj, E. and Kashani, M.M. (2022). "Nonlinear structural performance and seismic fragility of corroded reinforced concrete structures: modelling guidelines", *European Journal of Environmental and Civil Engineering*, 26(11), 5374-5403, https://doi.org/10.1080/19648189.2021.1896582.

Barron-Corvera, R. (2000). "Spectral evaluation of seismic fragility of structures" , State University of New York at Buffalo, Corpus ID: 15798216, http://civil.eng.buffalo.edu/~reinhorn/PUBLICATIONS/Reinhorn-Barron%20(2001)-%20ICOSSAR2001SpectP1.pdf.

Council, A.T. (2009). *Quantification of building seismic performance factors*, US Department of Homeland Security, FEMA, https://www.atcouncil.org/pdfs/FEMA-P695TOC.pdf.

Del Gaudio, C., De Risi, M.T., Ricci, P. and Verderame, G.M. (2019). "Empirical drift-fragility functions and loss estimation for infills in reinforced concrete frames under seismic loading", *Bulletin of Earthquake Engineering*, 17, 1285-1330, https://doi.org/10.1007/s10518-018-0501-y.

FEMA 356, F.E. (2000). "Prestandard and commentary for the seismic rehabilitation of buildings", Federal Emergency Management Agency: Washington, DC, USA, https://www.atcouncil.org/pdfs/FEMA356toc.pdf.

Gardner, L. (2019). "Stability and design of stainless steel structures-review and outlook", *Thin-Walled Structures*, 141, 208-216, https://doi.org/10.1016/j.tws.2019.04.019.

Ge, F.W., Tong, M.N. and Zhao, Y.G. (2021). "A structural demand model for seismic fragility analysis based on three-parameter lognormal distribution", *Soil Dynamics and Earthquake Engineering*, 147, 106770, https://doi.org/10.1016/j.soildyn.2021.106770.

Giordano, N., De Risi, R., Voyagaki, E., Kloukinas, P., Novelli, V., Kafodya, I., Ngoma, I., Goda, K.

and Macdonald, J. (2021). "Seismic fragility models for typical non-engineered URM residential buildings in Malawi", *Structures*, 32, 2266-2278, https://doi.org/10.1016/j.istruc.2021.03.118.

Goodarzi, M., Moradi, M., Jalali, P., Abdolmohammadi, M. and Hasheminejad, S. (2023). "Fragility assessment of an outrigger structure system based on energy method", *The Structural Design of Tall and Special Buildings*, 32(11-12), e2017, https://doi.org/10.1002/tal.2017.

Hancilar, U. and Caktı, E. (2015). "Fragility functions for code complying RC frames via best correlated im–edp pairs", *Bulletin of Earthquake Engineering*, 13, 3381-3400, https://doi.org/10.1007/s10518-015-9775-5.

Hosseinpour, F. and Abdelnaby, A. (2017). "Fragility curves for RC frames under multiple earthquakes", *Soil Dynamics and Earthquake Engineering*, 98, 222-234, https://doi.org/10.1016/j.soildyn.2017.04.013.

Housner, G.W. (1960). "The plastic failure of frame during earthquake", *Proceedings of 2nd WCEE*, VI, 997-1011, https://cir.nii.ac.jp/crid/1571135649126791296.

Jalayer, F., De Risi, R. and Manfredi, G. (2015). "Bayesian cloud analysis: Efficient structural fragility assessment using linear regression", *Bulletin of Earthquake Engineering*, 13, 1183-1203, https://doi.org/10.1007/s10518-014-9692-z.

Kircher, C.A., Whitman, R.V. and Holmes, W.T. (2006). "Hazus earthquake loss estimation methods", *Natural Hazards Review*, 7(2), 45-59, https://doi.org/10.1061/(ASCE)1527-6988(2006)7:2(45).

Liu, C., Fang, D. and Yan, Z. (2021). "Seismic fragility analysis of base isolated structure subjected to near-fault ground motions", *Periodica Polytechnica Civil Engineering*, 65(3), 768-783, https://doi.org/10.3311/PPci.15276.

Moradi, M. and Abdolmohammadi, M. (2020). "Seismic fragility evaluation of a diagrid structure based on energy method", *Journal of Constructional Steel Research*, 174, 106311, https://doi.org/10.1016/j.jcsr.2020.106311.

Moradi, M. and Tavakoli, H. (2020). "Proposal of an energy based assessment of robustness index of steel moment frames under the seismic progressive collapse", *Civil Engineering Infrastructures Journal*, 53(2), 277-293, https://doi.org/10.22059/ceij.2019.283574.1591.

Moradi, M., Tavakoli, H. and AbdollahZade, G. (2020). "Sensitivity analysis of the failure time of reinforcement concrete frame under postearthquake fire loading", *Structural Concrete*, 21(2), 625-641, https://doi.org/10.1002/suco.201900165.

Moradi, M., Tavakoli, H. and Abdollahzadeh, G. (2019). "Probabilistic assessment of failure time in steel frame subjected to fire load under progressive collapses scenario", *Engineering Failure Analysis*, 102, 136-147, https://doi.org/10.1016/j.engfailanal.2019.04.015.

Moradi, M., Tavakoli, H. and Abdollahzadeh, G.R. (2022). "Collapse probability assessment of a 4-story RC frame under post-earthquake fire scenario", *Civil Engineering Infrastructures Journal*, 55(1), 121-137, https://doi.org/10.22059/ceij.2021.313241.1718.

Moradpour, S. and Dehestani, M. (2021). "Probabilistic seismic performance of steel structures with FVDs designed by DDBD procedure", *Journal of Building Engineering*, 43, 102581, https://doi.org/10.1016/j.jobe.2021.102581.

Sharma, V., Shrimali, M.K., Bharti, S.D. and Datta, T.K. (2020). "Behavior of semi-rigid steel frames under near-and far-field earthquakes", *Steel and Composite Structures, an International Journal*, 34(5), 625-641, https://doi.org/10.12989/scs.2020.34.5.625.

Tavakoli, H. and Afrapoli, M.M. (2018). "Robustness analysis of steel structures with various lateral load resisting systems under the seismic progressive collapse", *Engineering Failure Analysis*, 83, 88-101, https://doi.org/10.1016/j.engfailanal.2017.10.003.

Tavakoli, H., Moradi, M., Goodarzi, M. and Najafi, H. (2022). "Outrigger braced system placement effect on seismic collapse probability of tall buildings", *Civil Engineering Infrastructures Journal*, 55(2), 259-276, https://doi.org/10.22059/ceij.2022.319629.1744.

Ugalde, D., Parra, P.F. and Lopez-Garcia, D. (2019). "Assessment of the seismic capacity of tall wall buildings using nonlinear finite element modeling", *Bulletin of Earthquake Engineering*, 17, 6565-6589, https://doi.org/10.1007/s10518-019-00644-x.

Xu, H. and Gardoni, P. (2016). "Probabilistic capacity and seismic demand models and fragility estimates for reinforced concrete buildings based on three-dimensional analyses", *Engineering Structures*, 112, 200-214, https://doi.org/10.1016/j.engstruct.2016.01.005.